DOI: 10.1111/j.1467-8659.2011.01948.x

Eurographics / IEEE Symposium on Visualization 2011 (EuroVis 2011)
H. Hauser, H. Pfister, and J. J. van Wijk
(Guest Editors)

Volume 30 (2011), Number 3

Visualization and Analysis of Eddies in a Global Ocean Simulation

S. Williams[1,2], M. Hecht[1], M. Petersen[1], R. Strelitz[1], M. Maltrud[3], J. Ahrens[1], M. Hlawitschka[2], and B. Hamann[2]

[1]Computer, Computational and Statistical Sciences Division, Los Alamos National Laboratory
[2]Institute for Data Analysis and Visualization (IDAV), Department of Computer Science, University of California, Davis
[3]Theoretical Division, Los Alamos National Laboratory

Abstract

We present analysis and visualization of flow data from a high-resolution simulation of the dynamical behavior of the global ocean. Of particular scientific interest are coherent vortical features called mesoscale eddies. We first extract high-vorticity features using a metric from the oceanography community called the Okubo-Weiss parameter. We then use a new circularity criterion to differentiate eddies from other non-eddy features like meanders in strong background currents. From these data, we generate visualizations showing the three-dimensional structure and distribution of ocean eddies. Additionally, the characteristics of each eddy are recorded to form an eddy census that can be used to investigate correlations among variables such as eddy thickness, depth, and location. From these analyses, we gain insight into the role eddies play in large-scale ocean circulation.

Categories and Subject Descriptors (according to ACM CCS): Computer Graphics [I.3.8]: Applications—Oceanography Simulation and Modeling [I.6.6]: Simulation Output Analysis—Ocean General Circulation Models

1. Introduction

Oceanography in the early and mid-20^{th} Century was focused on the description and analysis of the mean circulation. This changed later in the century as new observations produced evidence of a surprisingly vigorous field of often long-lived and deeply penetrating vortices, referred to as mesoscale eddies. Satellite-based sea surface height altimetry soon produced nearly global maps on which the surface signature of these vortices was clearly evident. Spectral analysis indicated that a large fraction of the total estimate of oceanic kinetic energy is associated with these mesoscale eddies [FS96], transforming our understanding of the fluid dynamics of ocean circulation.

Oceanic eddies are typically understood as vortices that are 50-200 km in diameter, may live for several months, and can propogate across an ocean basin. They are most numerous near strong currents like the Gulf Stream, Kuroshio Current, and Antarctic Circumpolar Current. These eddies have a significant influence on the earth's climate: they transport heat, freshwater, momentum, and mass [LBM02, VLF08]. The flow around eddies isolates the interior waters from the surrounding ocean; shipboard studies have measured higher concentrations of carbon, oxygen, and biologically important nutrients within eddies [MPH*07]. These nutrients are often transported by the eddies to nutrient-poor waters, increasing the productivity of the food chain.

Around the time that satellite-borne altimeters began producing near-global observations of sea surface height, ocean general circulation models (OGCMs) crossed into a higher resolution regime in which the mesoscale eddies began to be resolved. These models are closely related to those used in numerical weather prediction and atmospheric modeling in general, and the ancestry of the first OGCM [Bry69] owed a great deal to earlier work on numerical modeling of geophysical fluid dynamics for atmospheric science.

The first realistic eddying ocean model simulations focused regionally on the Southern Ocean [FRA91] and on the North Atlantic [BH89]. A spectral analysis of an approximately $\frac{1}{4}^{\circ}$ resolution model, based on the average horizontal spacing between grid points, showed a model sea surface height variability that was lower than that derived from the altimeter by approximately a factor of two [FS96]. As computing power increased, first regional and then global models could be configured and run at horizontal grid resolutions of around $\frac{1}{10}^{\circ}$, and their mesoscale variability was found to come into much better agreement with observa-

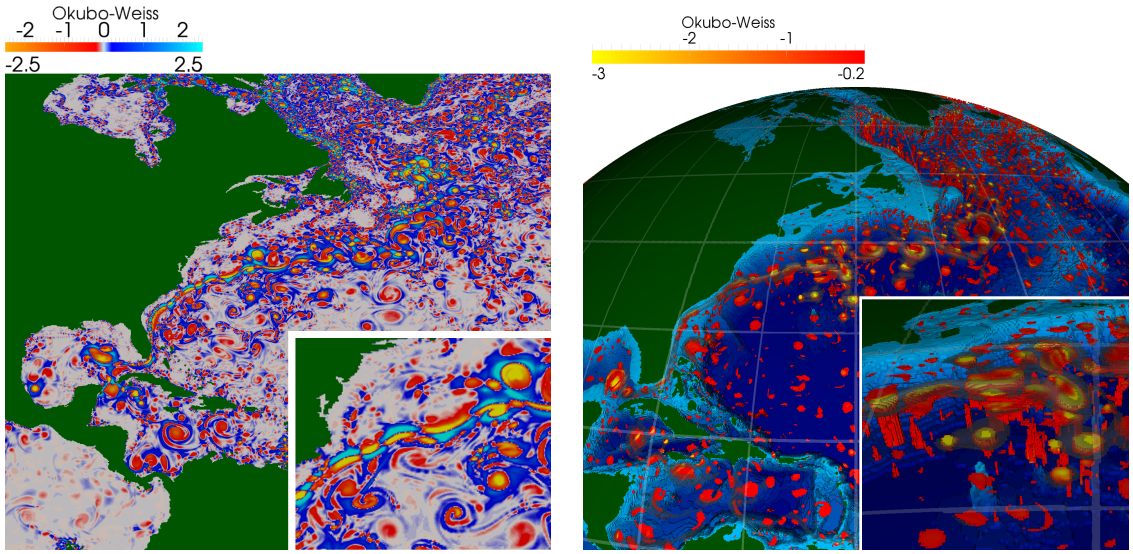

(a) (b)

Figure 1: (a) *The Okubo-Weiss parameter, a standard metric in oceanography for extracting two-dimenisonal vortices, at the ocean surface in the North Atlantic. In order to keep scaling consistent, the Okubo-Weiss value is normalized to its standard deviation. Red regions are those dominated by vorticity, while blue regions are those dominated by strain. The Okubo-Weiss parameter easily identifies several eddies as red circles, but non-eddy meanders in the Gulf Stream are detected as well.* (b) *The Okubo-Weiss parameter visualized at depth by removing all low-vorticity points. The three-dimensional shapes of the eddies are now made clear: in the region containing the Gulf Stream, several strong eddies reach very deeply into the ocean, while smaller eddies remain near the surface, and the Gulf Stream itself only dominates near the surface.*

tions [SMBH00, MM05]. The mean currents also came into much better agreement with observations in terms of width, speed and depth. The Gulf Stream, running from the Florida Straits and departing from the continental shelf at Cape Hatteras, then feeding into the northward-turning North Atlantic Current, showed great improvement in path, an indication of the essential role of eddy-mean flow feedbacks in determining the large scale circulation.

Computer modeling of ocean circulation and modern observing programs together have produced major advances in physical oceanography. Ocean models save full three-dimensional data fields, but publications in oceanography typically show simple two-dimensional plots of variables on the surface and in vertical sections. This is partly because oceanographers are familiar with these views from observational studies, and partly due to the limitations of the visualization tools that oceanographers typically use. Horizontal velocities in the ocean are 1000 times larger than vertical velocities, so 2D horizontal sections are often the best way to display the ocean's currents. A notable exception is the vertical structure of eddies. Questions about their vertical extent, tilt, and tapering require three-dimensional analysis and visualization.

To this end, we performed parallel analysis on high-resolution ocean simulation data on a local computing cluster, extracting eddies and visualizing them in the vicinity of one of the world's strongest ocean currents. Eddies are extracted by extending a standard vorticity metric to further distinguish circular flows from other spurious sources of high vorticity. Furthermore, by computing geometric information such as the thickness (distance from top to bottom) of every eddy across multiple daily snapshots of the simulation, we created histograms of eddy distribution and shape upon the two dimensions of a world map, providing a summarized global view of eddy characteristics. Finally, we use isolated geometric information from a single snapshot to create more detailed regional two- and three-dimensional maps to learn how eddy properties are related to each other and to the overall structure of the ocean. These analyses allow us to understand where thick, deeply penetrating eddies enable strong dynamical coupling of the upper and deep reaches of the ocean, and where biogeochemical activity will be locally enhanced or suppressed.

2. Related Work

Extracting and visualizing turbulence in vector fields has long been of interest to the visualization community [PVH*03, LHZP07]. Methods generally focus on either extracting specific structures (e.g., vortices) and drawing a bounding volume [SW97], or extracting the overall

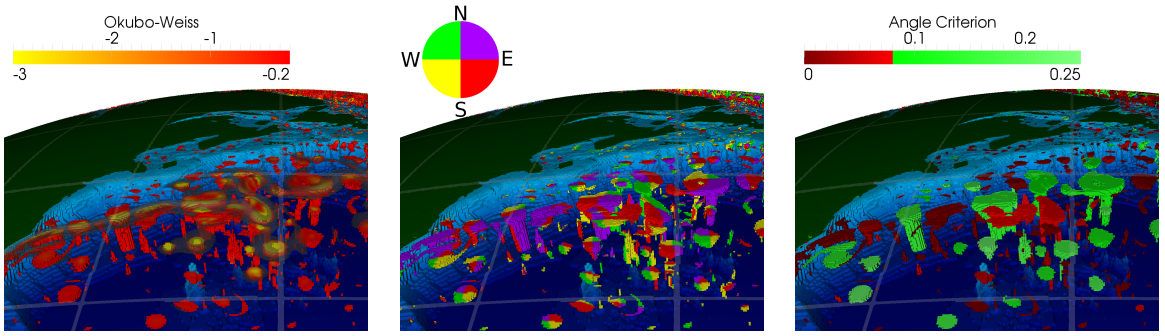

Figure 2: *High-vorticity features extracted from the North Atlantic. (a) Features are colored by Okubo-Weiss value, with high-speed water in translucent gray. Where the Gulf Stream turns, additional non-eddy but high-vorticity features appear. We would like to filter out these spurious features. (b) The same features, colored based on the angle each point's velocity vector makes with an east-pointing vector. Angles are discretized into four domains: angles between east and north (0° and 90°, colored purple), north to west (90° to 180°, green), west to south (180° to 270°, yellow), and south to east (270° to 360°, red). Features that are definitely eddies contain a nearly equal mixture of all four angle domains, while meanders move primarily in one or two directions and are dominated by one or two angle domains. (c) To use angle domains as a discriminator, we determine for each high-vorticity feature what percentage of its total volume is flowing in each angle domain. We consider only the minimum: if the feature is perfectly balanced between the four domains (eddy-like), the minimum percentage of any domain will be 25%. If the feature contains no points in a domain (non-eddy), its minimum percentage will be 0%. We determined experimentally that requiring a minimum of 8% (colored green) in each domain discriminates well between eddies and spurious high-vorticity features—so features colored green here pass the criterion, while features colored red do not.*

topology and visualizing it through glyphs or other proxies [HH91, TG09]. For extracting vortex-like structures in particular, popular methods include finding regions of high vorticity [VV92], streamline geometry [SP00] or, if the data are available, by looking for regions of low pressure at the center of a vortex [BS94].

One can also look for circular behavior in the velocity field directly. Jiang et al look at the problem topologically [JMT02], by looking for neighborhoods in which each vector in the neighborhood points in a unique direction range. Similarly, Sood et al [SJBT05] identify eddy centers by passing a 5×5 kernel of the angles between an east-pointing vector and the tangents of a circle centered in the kernel to find circular flows, then fitting an ellipse over the entire eddy. We employ a similar method to discriminate high-vorticity features, to attempt to separate eddies from non-eddy features.

In 3D visualization, Zhu and Moorhead [ZM95] extract eddies as a stack of 2D contours and stitch them together to show their 3D structure in the Pacific Ocean off the coast of Japan. They develop a new extraction technique, but the restrictiveness of their method appears to preclude extracting deep eddies, which have been observed to exist in that region. Grant et al [GEO02] developed a method for fitting a surface to the thermocline—the interface between the upper, well-mixed ocean and the deep, stratified ocean. His visualizations show quite clearly the perturbations that eddies can cause in the thermocline.

Several techniques have also been developed to further refine analysis of the vorticity field. We use the Okubo-Weiss criterion [Oku70, Wei91], which is known in the visualization community as the Q criterion [HWM88]. This criterion highlights areas where vorticity dominates strain. Also of note is the λ_2 criterion [JH95], that uses the second eigenvalue of the strain tensor times the sum of the squares of strain and vorticity to determine whether vorticity or strain are dominant in a region. We chose the Okubo-Weiss criterion over λ_2 because it is the standard vortex criterion within the oceanographic community.

Numerous studies of satellite data have quantified the size and distribution of oceanic eddies, mostly based on consideration of the Okubo-Weiss parameter. Published works have considered regions including the Mediterranean Sea [IFGLFGO06], the Tasman Sea [WAB06], the Gulf of Alaska [HT08] and the full nearly-global domain of all but the ice-covered seas [CSSdS07].

An eddy census from satellite data is limited to surface features, while data from vertical ship-deployed profiles and fixed moorings are sparse and can only capture a very incomplete picture. Ocean models have been used as a means to study features that are not directly observable at this time, and therefore to fill in our understanding of the oceans. Much of the knowledge of so-called eddy transports of heat, salt

and nutrients has been derived from the analysis of ocean models [JM02, YNQ*10]. It is important to note that the discussion of eddy transport in the literature generally refers to all transport not explicitly accounted for in the mean flow, which will include any temporal variability in the mean flow, such as the slow meandering of large-scale currents.

Eddies are understood to provide a principal means of coupling between the circulations of the upper and deep ocean [HL75, HH08]. The vertical structure of eddies is also understood to influence the suppression or enhancement of biogeochemical activity through their control over nutrient supply through the base of the euphotic zone (the zone over which light penetration is sufficient to support photosynthesis). It has been shown that the effect on nutrient supply and biological activity can be of opposite sign depending on whether the eddy is a thick one of low vertical mode structure or a thin one of higher vertical mode [AMM*10], motivating our classification of eddies into thick and thin.

3. Methods

Our analysis of eddies focuses on data generated by Los Alamos National Laboratory's Parallel Ocean Program (POP) [SDM92] in the context of a global ocean simulation with grid resolution of approximately $\frac{1}{10}^{\circ}$. As explained in [MBH*08, MBP10], the horizontal grid follows lines of latitude and longitude in the southern hemisphere, where the landmass of the Antarctic continent prevents the singularity in latitudinal spacing that occurs at the South Pole (where all grid points would share the same southern neighbor, turning rectangular grid cells into triangles) from imposing an otherwise severe time step limitation on the finite volume discretization of the ocean model. In the northern hemisphere, where the northern pole is in the middle of an ocean basin, a more complex discretization is used in order to maintain relatively uniform grid cell areas with horizontal aspect ratios that do not deviate greatly from one. This is accomplished using a tripole grid, in which two North Poles are used instead, with one located in Canada and the other in Siberia. In such a grid, the top row of points forms a line from one pole to the other and back again, and any degenerate cells occur on land and are ignored by the simulation.

Oceanic flows take on extreme aspect ratios when considered in three dimensions, with horizontal scales being orders of magnitude larger than characteristic vertical scales. Whereas $\frac{1}{10}^{\circ}$, or approximately 10 km, is considered extremely fine horizontal resolution, the vertical resolution is much higher, with grid spacing on the order of 10 m near the surface, reaching 250 m in the deep ocean, with a smooth transition between. The model output is then a rectilinear grid of size $3600 \times 2400 \times 42$. These data comprise approximately 1.4 GB per floating-point variable per daily snapshot, so all our visualization and analysis was done on a local thirty-two core cluster primarily using the visualization toolkit ParaView. We consider two input variables from the simulation, comprising the two components of horizontal velocity. The vertical velocity does not contribute significantly to the relative vorticity, being several orders of magnitude smaller in scale than the horizontal velocity, as is characteristic of geophysical flows. Any points that lie in land are assigned a special value of -10^{34} in all fields, so the bathymetry (a depth map of the bottom of the ocean) can be readily inferred.

While the details of the grid are specific to a run of POP—the simulation code supports different methods for removing the northern pole singularity, like keeping a single North Pole but moving it so it lies in Canada—one of the inputs to the POP run (that is similarly available as input to us) is a mapping from grid coordinates to longitude and latitude. The mapping is simply a two-dimensional rectilinear grid of size 3600×2400, noting that all points at a particular (i, j) grid coordinate (i.e., at any depth) share the same longitude and latitude. This creates a spherical coordinate system of longitude, latitude, and r as the distance from the center of the Earth (computed as the radius of the Earth, 6,371 km, minus the depth of the point in the simulation grid) that can be easily transformed into Cartesian coordinates for making the Earth-like visualizations in figures 1 and 2. In these visualizations, depth is exaggerated by a factor of 50, because with three orders of magnitude separating the radius of the Earth (6,371 km) from the maximum depth of POP (about 6 km), depth-dependent features (including the bathymetry of the ocean) are imperceptibly small without exaggeration.

3.1. Eddy Extraction

We begin with one of the ocean community's canonical methods for identifying eddies: the Okubo-Weiss parameter. We chose to start with this metric because, while it certainly is not the only means of identifying vortical features, its popularity among oceanographers puts this work in a context that can be immediately understood by members of the ocean community. In general, this parameter divides the ocean into regions dominated by vorticity, regions dominated by strain or deformation, and a background where neither effect is dominant. Regions dominated by vorticity are potentially eddies, though vorticity dominance can be caused by other effects, such as sharp turns in the mean flow. Mathematically, the Okubo-Weiss parameter is defined as:

$$OW = s_n^2 + s_s^2 - \omega^2 \tag{1}$$

Here, s_n is normal strain (currents pushing against each other), s_s is shear strain (currents running in opposite directions past each other), and ω is vorticity (currents moving in circles). These three variables can be expressed in terms of velocity gradients:

$$s_n = \frac{\partial u}{\partial x} - \frac{\partial v}{\partial y} \quad (2)$$

$$s_s = \frac{\partial v}{\partial x} + \frac{\partial u}{\partial y} \quad (3)$$

$$\omega = \frac{\partial v}{\partial x} - \frac{\partial u}{\partial y} \quad (4)$$

Here, u refers to the east-west velocity component, and v to the north-south velocity component. Then, x and y are locally east-pointing and north-pointing vectors, respectively. (We assume that within a single grid cell, which is about 11km on a side at the equator and smaller at higher latitudes, the curvature of the Earth is negligible. Thus, we consider the local coordinate system at each simulation point coplanar with the local manifold of the Earth.) Substituting these gradients into the original Okubo-Weiss expression provides an equation that can be solved solely from velocity:

$$OW = \left(\frac{\partial u}{\partial x} - \frac{\partial v}{\partial y}\right)^2 + \left(\frac{\partial v}{\partial x} + \frac{\partial u}{\partial y}\right)^2 - \left(\frac{\partial v}{\partial x} - \frac{\partial u}{\partial y}\right)^2 \quad (5)$$

Being defined only in terms of velocity gradients, the Okubo-Weiss parameter has the advantage of being entirely local and as a result it scales well to large data. A first approach to visualizing the Okubo-Weiss parameter might be to consider the parameter solely in terms of positive (strain-dominated) and negative (vorticity-dominated) domains, but for numbers close to zero the parameter is dominated by noise. To select only vorticity-dominated features, then, we need to apply a threshold to only retain points with negative Okubo-Weiss values, but due to the parameter being noisy for very low values, the threshold should be nonzero. The convention in the ocean community is to divide the Okubo-Weiss value by its standard deviation (normalizing it such that -1 is one standard deviation left of the mean) to provide relatively data-independent scaling of its values, and only consider a data point meaningful if it is at least 0.2 standard deviations from 0 (i.e., remove all points with Okubo-Weiss above -0.2). We follow this convention, to ensure that our starting point for eddy analysis is consistent with the baseline assumptions of prior oceanographic studies of eddies.

The Okubo-Weiss parameter is plotted at the ocean surface in Figure 1a. For this study we are interested in eddies as discrete entities (i.e., seeing the strict boundary of eddies according to our definition), so we believe volume rendering would be inappropriate as a visualization technique. Instead we employ a threshold to keep only points with negative Okubo-Weiss values at least 0.2 standard deviations from 0, and render them as solid cubes. We further place these extracted eddies on a bathymetric map also extracted from the simulation data to geographically orient viewers and to show the interaction between deep eddies and the ocean floor. The resulting visualization is shown for the North Atlantic's Gulf Stream in Figure 1b.

From this point forward, eddies (or more precisely, high-vorticity features) are defined as connected components of points that all have Okubo-Weiss values below -0.2 standard deviations. Considering that POP lies on a rectilinear grid, we define two points as neighbors if their voxels (the actual volume the points represent) share a face. More colloquially, this is six-way adjacency: each interior point has six neighbors, so if a point is indexed by (i, j, k), then its neighbors are $(i+1, j, k)$, $(i-1, j, k)$, $(i, j+1, k)$, $(i, j-1, k)$, $(i, j, k+1)$, and $(i, j, k-1)$.

These pictures indicate that, while the Okubo-Weiss parameter identifies eddies both at and below the surface of the ocean, it also identifies high-vorticity features that should not be considered eddies, particularly meanders in the Gulf Stream and other strong currents around the world, as well as several small-scale features that we consider noise. To mitigate this, we have added one more filtering criterion. We compute the angle between each point's velocity vector and a vector pointing east. These angles are discretized into four domains: 0 to 90 degrees (northeast), 90 to 180 degrees (northwest), 180 to 270 degrees (southwest), and 270 to 360 degrees (southeast). Figure 2b shows the same vorticity-dominated features as Figure 2a, but recolored to show the angle domain each point falls within.

Since an eddy is a circular flow, we expect that an eddy should contain velocity vectors in all four angle domains, and that its center point should be at the intersection of these four domains. Indeed, the vorticity-dominated regions of the Gulf Stream that are most likely eddies do show a cross-shaped pattern in their angle domains, indicating that the current is circling around the center of the eddy. However, several of the larger meanders also contain all four angle domains, either due to making a sufficiently sharp hairpin turn, or by making S-shaped turns. Instead, for using these angle domains to discriminate between eddies and other features, we require that each angle domain make up at least a certain share of the total eddy, as shown in Figure 2c. Based on experimentation, we arrived at a requirement of 8%.

As our eddy extraction was implemented using ParaView, the computation is parallelized by breaking the data apart into roughly equally-sized blocks. Besides projecting velocity from grid space to world space to correct for the distortions introduced by the tripole coordinate system, computing the Okubo-Weiss parameter is primarily dependent on computing velocity gradients. We apply central differencing to find approximate gradients, which is a function on up to six neighbors. In order to further regularize the data across time, we choose the same normalization factor for the entire data set: the standard deviation of Okubo-Weiss at the ocean surface on the vernal equinox (March 21). We use a single normalization factor for all time steps to ensure that the magnitude of Okubo-Weiss is directly comparable between time

steps. We then use ParaView's threshold filter to remove all points with Okubo-Weiss above -0.2σ, leaving only high-vorticity features behind. At this point, the angle between each point's velocity vector and an east-pointing vector is computed from simple trigonometry, and discretized into one of the four domains as above.

After the threshold filter is applied, ParaView automatically converts the data to an unstructured grid with the same connectivity implicit in the rectilinear grid and, since the threshold automatically breaks connectivity between unconnected eddies (because the points connecting the eddies have been removed), eddies can be identified with a breadth-first search. The final implementation consideration is that in dividing the data, it is quite likely for some eddies to be split across two processes. In that case, since a breadth-first search in one process would not automatically cross the process boundary, the split eddy would be represented as two independent eddies, causing the eddy to be either double-counted, or more likely, making it too dominant in one or two angle domains and fail to pass our angle criterion.

There are two obvious solutions: employ message passing between the processes, or have the boundaries overlap by at least the size of the largest eddy. We opted for the latter solution, since then each eddy automatically resides entirely in at least one process. Specifically, each process has a certain block assigned to it, with points assigned uniquely to blocks and all points in exactly one block, and each process also takes an overlap region into its neighboring blocks such that, while each point is uniquely claimed, it can appear in the overlap region of up to three other processes. Finally, since that implies that an eddy in the overlap region will reside in part or in whole in at least two processes, a process is only allowed to claim an eddy if the point with minimum Okubo-Weiss is not in its overlap region. The only caveat to this definition is that it assumes a unique minimum Okubo-Weiss value per eddy, further subject to the vagaries of floating-point numbers, though floating-point imprecision has not appeared to be a problem in practice. While it might also appear to be a problem that one process might not have the point with minimum Okubo-Weiss value in either its main block or its overlap zone, we assume that the overlap zone is at least as large as the largest eddy. If a point from an eddy is not contained anywhere in the data available to a specific process, then the eddy must touch a border and therefore reside entirely in the overlap zone, so it cannot be claimed by that process.

3.2. Census and Analysis

In addition to visualizing ocean eddies directly, we also developed a capability to analyze the distribution, size, thickness, and depth of eddies around the world. We consider the following computed quantities for each eddy:

- Volume: computed as sum of the volumes of all voxels in the eddy, with voxels approximated as cubes (though in reality they would be rectangular solid angles of a spherical shell)
- Radius: we consider the radius (the radial extent of an eddy in a latitude-longitude manifold, i.e., in a plane normal to the surface of the Earth) with respect to the depth containing the most negative (i.e., strongest) Okubo-Weiss value; at this depth, the radius is approximated by computing the area of the eddy at that depth as the sum of the areas of all voxels (computed as the longitudinal extent times the latitudinal extent), then by assuming the eddy is a circle at this depth, taking $r = \sqrt{A/\pi}$
- Thickness: computed as the maximum difference between the depths of any two points in the eddy
- Vorticity sign: positive if at least half the points in the eddy have positive vorticity (spin counterclockwise), and negative otherwise

Visualizations like those in the previous section are only useful for looking at snapshots of isolated regions of the ocean, due to the density of information being displayed. Here we synthesize 350 global snapshots of daily data to create an eddy census database in order to study the statistical distributions of eddy metrics.

To generate the census, the world is broken into bins 1° on each edge. One statistic we highlight is a count: for each snapshot, the number of eddies in each bin is counted, then each bin's count is averaged across the 350 available daily snapshots. This census, in Figure 3c, shows strong eddy activity in the Gulf Stream in the western Atlantic Ocean, the Kuroshio Current in the western Pacific Ocean, and the Antarctic Circumpolar Current ringing Antarctica in the Southern Ocean. Additionally, because of the simplicity of the statistics in this image, it can easily be qualitatively compared to observational data to confirm its validity. In Figures 3a and 3b we use model and satellite altimetry data to derive sea surface height variability, or, the difference between instantaneous and averaged sea surface height. The principle observation is that eddies cause bulges on the surface of the ocean. Averaging the sea surface height over a large amount of time removes the temporary bulges caused by eddies (providing the sea surface height due to mean flow). Then, the difference between the average and instantaneous sea surface height highlights behavior not attributable to the mean flow, e.g., eddies. Using this approach shows regions of observed strong surface eddy activity, which correspond fairly well to the eddy activity regions found by our census.

The surface characteristics of eddies are well known from satellite observations, but the depth of penetration has been less adequately observed. With model data we can measure average eddy thickness, or the distance from the top of the eddy to the bottom. Figure 3d reveals several thick eddies in the midst of the Gulf Stream, Kuroshio Current, and Antarctic Circumpolar Current. Focusing on the Atlantic, there are significant numbers of eddies with depths on the order of

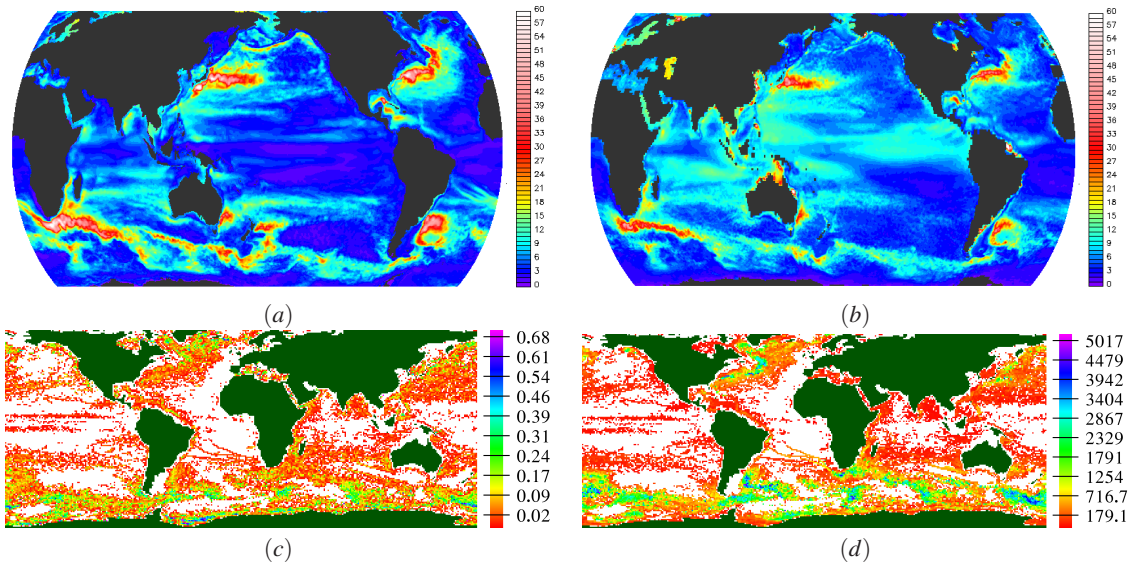

Figure 3: *Sea surface height variability in centimeters, defined as the root mean square of the difference between the instantaneous height of the sea surface and its time-mean, can be used as a proxy measurement for eddy activity. To compare model to observational data directly, we first show sea surface height variability from* (*a*) *POP ocean model data and* (*b*) *observational data from the AVISO processing of satellite altimetry. In these images, the simulation shows exceptionally good agreement to observation.* (*c*) *Our global eddy census, showing the average number of eddies per* 1° *of latitude and longitude, averaged across 350 daily snapshots. Note that the color bar of* (*c*) *is reversed relative to that of* (*a*) *and* (*b*)*. Relating the numerical density of eddies in* (*c*) *to sea surface height variability, both measures indicate high levels of eddy activity in the same locations.* (*d*) *Average eddy thickness in meters as a function of latitude and longitude. We use thickness to refer to the distance from the top of an eddy to the bottom. Notably, thick eddies only have a significant signal in the regions of the same three big currents, the Gulf Stream, Kuroshio Current, and Antarctic Circumpolar Current, where they can get as thick as 5000m.*

5000m. This means that some eddies extend from the surface of the ocean to the floor, and several more stretch half the maximum height of the ocean.

Oceanographers would like to know which eddies are confined to the upper ocean, which extend into the deep ocean, and if there are isolated deep eddies without surface features. The upper ocean is well mixed due to wind-induced waves and turbulence, while the deep ocean is stratified with little vertical mixing. The thermocline—a surface at the depth where temperature changes more rapidly—lies somewhere between these two regions of lower vertical temperature gradient, and serves as a depth to separate shallow eddies from deep eddies in our analysis.

Figure 4a shows a skeletonized view of the region of the northwest Atlantic we identified from Figure 3d as likely to contain thermocline-penetrating eddies. Eddy skeletons are drawn as a cylinder vertically spanning the thickness of the eddy (so the top of the cylinder is at the same depth as the highest point in the eddy, and the bottom of the cylinder is at the same depth as the lowest point in the eddy), and the cylinder passes through the most vortical point in the eddy (where the Okubo-Weiss value is most negative). The cylinders are drawn with fixed radius to avoid providing overwhelming amounts of information, as this visualization contains all the information we need to address the question under consideration. Even from this simplified view it is visually apparent that there are several eddies beginning near the surface of the ocean and extending down quite far, but to make the relationship more explicit, we created a two-dimensional map showing where thermocline-penetrating eddies occur. Eddies that penetrate the thermocline, meaning that they begin above the thermocline and end below it, are shown as blue squares if they spin counterclockwise, and red squares if they spin clockwise. Eddies entirely above or below the thermocline are represented by gray diamonds. For this map, we use an estimate of the thermocline depth of 700m [AMM*10].

4. Results

Our results were reviewed by three Los Alamos National Laboratory scientists specializing in ocean modeling—Matthew Hecht, Mark Petersen, and Mat Maltrud—who drew a number of insights from these visualizations. Their consideration of results begins with Figure 2c, where discrimination has been performed in order to separate mesoscale eddies from other high-vorticity features. In this view of the northwest Atlantic the deeper eddies tend to be

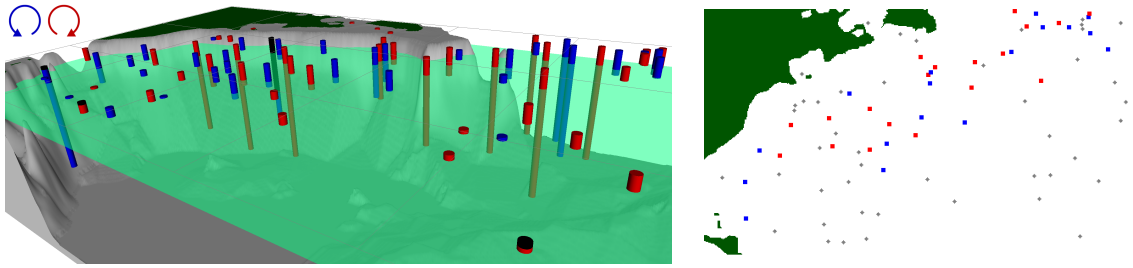

(a) (b)

Figure 4: (a) *Skeletonized view of the eddy field in the northwest Atlantic, from* -80° *to* -30° *longitude and* 20° *to* 50° *latitude. Eddies are pictured as blue or red cylinders of vertical extent, with black lines projecting subsurface eddies onto the ocean surface to aid in visual alignment. Blue eddies have positive vorticity (counterclockwise spin), while red eddies have negative vorticity (clockwise spin). The green translucent layer approximates the thermocline.* (b) *Two-dimensional map of the same eddy field. Eddies that penetrate the thermocline (i.e., that have their minimum depth above the thermocline and their maximum depth below) are represented as colored boxes; these are the eddies that can couple the upper and deep ocean. Coloration is the same used in the skeletonized view: blue for counterclockwise and red for clockwise. Eddies that exist entirely above or below the thermocline are gray diamonds. For this region of the Atlantic, the thermocline is at about 700m [AMM*10].*

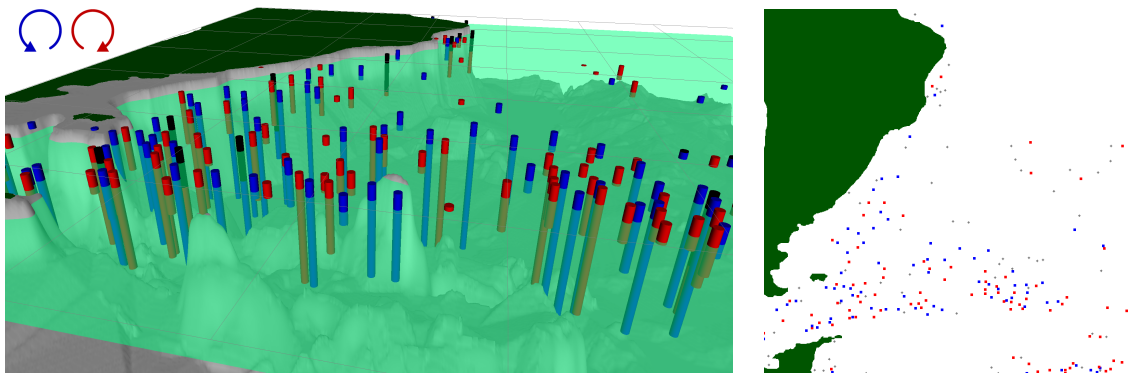

(a) (b)

Figure 5: (a) *Skeletonized view of the eddy field in the Southern Atlantic, from* -70° *to* 0° *longitude and* -70° *to* 0° *latitude. The thermocline in this region of the ocean is taken to be 500m.* (b) *Two-dimensional map of the same eddy field.*

associated with the Gulf Stream, where some of them have been formed through a process in which meanders in the Stream become rings and then pinch off from the main flow. All of these deep eddies derive their kinetic energy mainly through the release of potential energy in the upper ocean, but the depth to which the eddies penetrate enables a transfer of energy to the deep ocean. Figure 3d shows the spatial distribution of these deep eddies that explain the eddy-driven circulation of the abyssal ocean, as anticipated in the idealized but highly influential work of [HL75].

Most of the eddies in the interior foreground of Figure 2c, south of the path of the Gulf Stream, are thin and shallow. In this region of the North Atlantic surrounding Bermuda, referred to as the Sargasso Sea, it has been shown that the tendency of eddies to either enrich or suppress nutrient supply depends not only on the rotational orientation of the eddy (counter-clockwise versus clockwise, or in geophysical terms, cyclonic versus anti-cyclonic), but also depends on whether the eddy is thick or thin, with the sign of the effect being reversed if the eddy is thin rather than thick [AMM*10]. These two criteria of rotational orientation and thickness are shown more clearly in the skeletonized view of Figure 4a. [AMM*10] goes on to make the structural distinction between thin and thick eddies based on whether the eddy penetrates the thermocline, where higher vertical temperature gradients exist at intermediate depth somewhere between the well mixed waters near the surface and the weak gradients of the deep ocean. In Figure 4b we distinguish, eddy-by-eddy, between those that are thin and those that are thick enough to cross the thermocline (being represented by colored squares in the two-dimensional map).

A similar analysis in Figure 5 of the depth distribution of

eddies in the Southern Ocean, where the powerful Antarctic Circumpolar Current circles the Earth nearly unimpeded by land masses, shows a remarkable concentration of deep eddies that pass our detection criteria to the bottom of the ocean. It should be noted that for numerical reasons (i.e., how many points are required to get 8% in each angle domain relative to the total number of points) our detection criteria is stricter in a relative sense in the deep ocean, as compared with the upper ocean, because deep ocean velocities tend to be smaller. It seems likely that these particularly intense eddies have been "pinched off" as meanders in the flanks of the Current. The formation process will be examined once our techniques have been extended in a robust way to the tracking of individual three-dimensional eddies through time.

The great abundance of thick eddies in the Southern Ocean, along the path of the Antarctic Circumpolar Current, is also very apparent in Figure 3d. It has recently been argued, again based on idealized study, that the eddies of the Southern Ocean set the stratification of the much of the World Ocean [WC10]. Our visualizations show that there is a vast array of deep eddies spanning the southern extremes of the Pacific, Atlantic and Indian sectors, capable of exerting control over the mid-depth stratification of the World Ocean.

Another area in which particularly deep-reaching eddies appear in Figure 3d is where the westward-flowing Agulhas Current has its "retroflection." This occurs off the southern tip of Africa, where most of the waters of the Agulhas Current reverse course to become swept up with the eastward-flowing Antarctic Circumpolar Current, and deep eddies sporadically break off of the powerful Agulhas Current. This sends masses of Indian Ocean waters spinning off into and across the South Atlantic where they modulate the strength of the Atlantic overturning circulation [BBL08]. The Gulf Stream region is also closely associated with the overturning circulation, with its downstream manifestation, the North Atlantic Current, believed to have taken a different course at the time of the Last Glacial Maximum [RMM95], and this is another region of notably deep eddies. This is also a region in which a particularly vigorous deep circulation appears to be driven by vertical momentum transfer through the eddy field. In turn, the deep circulation interacts strongly with the circulation of the upper ocean, controlling the path of the Gulf Stream, in a delicate and entirely mutual interaction between upper and lower components of the circulation [HH08].

5. Conclusion

The complete role of deep, thermocline-penetrating eddies is not currently well understood. Partly this is because observational data at depth are sparse, and global ocean simulations have only recently reached the resolutions required to reliably resolve eddies. We began addressing this by extracting eddies from a tenth-degree global ocean simulation, starting from the standard Okubo-Weiss parameter. Because the Okubo-Weiss parameter identifies any feature where vorticity dominates strain, we created a new criterion to select for circular, more eddy-like vorticity features. From there, we gathered statistical data about the global eddy field across 350 daily snapshots and visualized them in a summarized world map of characteristics and distributions, and used statistics from a single snapshot to make detailed geographical and correlative visualizations of the eddies' properties.

To this end, we intend to expand our analytical capabilities to include eddy tracking over time, and to allow for more extensive three-dimensional consideration of correlations with additional variables including temperature, salinity, potential density and enstrophy.

Acknowledgements

This work was supported by the Department of Energy (DOE) Office of Science (OSC) Biological and Environmental Research (BER) Climate Visualization Program, the LANL-UC Davis Materials Design Institute, and in part by NSF grant CCF-0702817. Finally, we thank the members of the Institute for Data Analysis and Visualization (IDAV), Department of Computer Science, UC Davis, and the Applied Computer Science group at Los Alamos National Laboratory.

References

[AMM*10] ANDERSON L. A., MCGILLICUDDY, JR. D. J., MALTRUD M. E., LIMA I. D., DONEY S. C.: Impact of eddy-wind interaction on eddy demographics and phytoplankton community structure in a model of the North Atlantic Ocean. *Dyn. Atmos. Oceans* (2010), submitted. 4, 7, 8

[BBL08] BIASTOCH A., BÖNING C. W., LUTJEHARMS J.: Agulhas leakage dynamics affects decadal variability in Atlantic overturning circulation. *Nature 456* (2008), 489–492. 9

[BH89] BRYAN F., HOLLAND W.: A high-resolution simulation of the wind- and thermohaline-driven circulation in the North Atlantic Ocean. In *Proceedings of the 'Aha Huliko'a Hawaiian Winter Workshop*, Muller P., Henderson D., (Eds.), Hawaii Inst. Geophys. Spec. Publ. U. Hawaii, 1989, pp. 99–115. 1

[Bry69] BRYAN K.: A numerical method for the study of the circulation of the World Ocean. *J. Comput. Phys.4* (1969), 347—376. 1

[BS94] BANKS D. C., SINGER B. A.: Vortex tubes in turbulent flows: identification, representation, reconstruction. In *VIS '94: Proceedings of the conference on Visualization '94* (Los Alamitos, CA, USA, 1994), IEEE Computer Society Press, pp. 132–139. 3

[CSSdS07] CHELTON D. B., SCHLAX M. G., SAMELSON R. M., DE SZOEKE R. A.: Global observations of large oceanic eddies. *Geophysical Research Letters 34*, L15606 (2007), 5. 3

[FRA91] FRAM GROUP: An eddy-resolving model of the Southern Ocean. *EOS Trans. AGU72* (1991), 169–175. 1

[FS96] FU L. L., SMITH R. D.: Global ocean circulation from satellite altimetry and high-resolution computer simuation. *Bull. Amer. Meteorol. Soc.11*, 77 (1996), 2625–2636. 1

[GEO02] GRANT J., ERLEBACHER G., O'BRIEN J.: Case study: Visualizing ocean flow vertical motions using lagrangian-eulerian time surfaces. In *Visualization, 2002. VIS 2002. IEEE* (Nov. 2002), pp. 529 –532. 3

[HH91] HELMAN J. L., HESSELINK L.: Visualizing vector field topology in fluid flows. *IEEE Comput. Graph. Appl. 11*, 3 (1991), 36–46. 3

[HH08] HURLBURT H. E., HOGAN P. J.: The Gulf Stream pathway and the impacts of the eddy-driven abyssal circulation and the Deep Western Boundary Current. *Dyn. Atmos. Oceans 45* (2008), 71–101. 4, 9

[HL75] HOLLAND W. R., LIN L. B.: On the generation of mesoscale eddies and their contribution to the oceanic general circulation. I. A preliminary numerical experiment. *J. Phys. Oceanogr.5*, 4 (1975), 642 – 57. 4, 8

[HT08] HENSON S. A., THOMAS A. C.: A census of oceanic anticyclonic eddies in the gulf of alaska. *Deep Sea Research Part I: Oceanographic Research Papers 55*, 2 (2008), 163 – 176. 3

[HWM88] HUNT J. C. R., WRAY A. A., MOIN P.: Eddies, streams, and convergence zones in turbulent flows. In *Studying Turbulence Using Numerical Simulation Databases, 2* (Dec. 1988), pp. 193–208. 3

[IFGLFGO06] ISERN-FONTANET J., GARCÍA-LADONA E., FONT J., GARCÍA-OLIVARES A.: Non-gaussian velocity probability density functions: An altimetric perspective of the mediterranean sea. *J. Phys. Oceanogr.36*, 11 (2006), 2153 – 2164. 3

[JH95] JINHEE JEONG, HUSSAIN F.: On the identification of a vortex. *Journal of Fluid Mechanics 285* (25 February 1995), 69–94. 3

[JM02] JAYNE S. R., MAROTZKE J.: The oceanic eddy heat transport*. *Journal of Physical Oceanography 32*, 12 (2002), 3328–3345. 4

[JMT02] JIANG M., MACHIRAJU R., THOMPSON D.: A novel approach to vortex core region detection. In *Proceedings of the symposium on Data Visualisation 2002* (Aire-la-Ville, Switzerland, Switzerland, 2002), VISSYM '02, Eurographics Association, pp. 217–ff. 3

[LBM02] LEACH H., BOWERMAN S. J., MCCULLOCH M. E.: Upper-ocean eddy transports of heat, potential vorticity, and volume in the northeastern north atlantic—"vivaldi 1991". *Journal of Physical Oceanography 32*, 10 (2002), 2926–2937. 1

[LHZP07] LARAMEE R., HAUSER H., ZHAO L., POST F.: Topology-based flow visualization, the state of the art. In *Topology-based Methods in Visualization*, Hauser H., Hagen H., Theisel H., (Eds.), Mathematics and Visualization. Springer Berlin Heidelberg, 2007, pp. 1–19. 10.1007/978-3-540-70823-0_1. 2

[MBH*08] MALTRUD M., BRYAN F., HECHT M., HUNKE E., IVANOVA D., MCCLEAN J., PEACOCK S.: Global ocean modelling in the eddying regime using POP. *CLIVAR Exchanges 44*, 1 (January 2008), 5–8. (unpublished manuscript). 4

[MBP10] MALTRUD M., BRYAN F., PEACOCK S.: Boundary impulse response functions in a century-long eddying global ocean simulation. *Environmental Fluid Mechanics 10*, 1-2 (APR 2010), 275–295. 4

[MM05] MALTRUD M. E., MCCLEAN J. L.: An eddy resolving $1/10^{\circ}$ ocean simulation. *Ocean Modelling8*, 1–2 (2005), 31–54. 2

[MPH*07] MATHIS J. T., PICKART R. S., HANSELL D. A., KADKO D., BATES N. R.: Eddy transport of organic carbon and nutrients from the Chukchi Shelf: Impact on the upper halocline of the western Arctic Ocean. *Journal of Geophysical Research (Oceans) 112*, C11 (May 2007), 5011. 1

[Oku70] OKUBO A.: Horizontal dispersion of floatable particles in the vicinity of velocity singularities such as convergences. *Deep Sea Research and Oceanographic Abstracts 17*, 3 (1970), 445 – 454. 3

[PVH*03] POST F. H., VROLIJK B., HAUSER H., LARAMEE R. S., DOLEISCH H.: The state of the art in flow visualisation: Feature extraction and tracking. *Computer Graphics Forum 22*, 4 (2003), 775–792. 2

[RMM95] ROBINSON S. G., MASLIN M. A., MCCAVE I. N.: Magnetic-susceptibility variations in Upper Pleistocene deep-sea sediments of the NE Atlantic – Implications for ice rafting and paleocirculation at the Last Glacial Maximum. *Paleoceanography 10*, 2 (1995), 221 – 250. 9

[SDM92] SMITH R. D., DUKOWICZ J. K., MALONE R. C.: Parallel ocean general circulation modeling. *Physica D: Nonlinear Phenomena60* (1992), 38—61. 4

[SJBT05] SOOD V., JOHN B., BALASUBRAMANIAN R., TANDON A.: Segmentation and tracking of mesoscale eddies in numeric ocean models. In *Image Processing, 2005. ICIP 2005. IEEE International Conference on* (September 2005), vol. 3, pp. III – 469–72. 3

[SMBH00] SMITH R. D., MALTRUD M. E., BRYAN F. O., HECHT M. W.: Numerical simulation of the North Atlantic Ocean at $\frac{1}{10}^{\circ}$. *J. Phys. Oceanogr.30* (2000), 1532–1561. 2

[SP00] SADARJOEN I. A., POST F. H.: Detection, quantification, and tracking of vortices using streamline geometry. *Computers & Graphics 24*, 3 (2000), 333 – 341. 3

[SW97] SILVER D., WANG X.: Tracking and visualizing turbulent 3d features. *Visualization and Computer Graphics, IEEE Transactions on 3*, 2 (apr. 1997), 129 –141. 2

[TG09] TRICOCHE X., GARTH C.: Topological methods for visualizing vortical flows. In *Mathematical Foundations of Scientific Visualization, Computer Graphics, and Massive Data Exploration*, Farin G., Hege H.-C., Hoffman D., Johnson C. R., Polthier K., Rumpf M., (Eds.), Mathematics and Visualization. Springer Berlin Heidelberg, 2009, pp. 89–107. 10.1007/b106657_5. 3

[VLF08] VOLKOV D. L., LEE T., FU L.: Eddy-induced meridional heat transport in the ocean. *Geophys. Res. Lett.35* (Oct. 2008), 20601–+. 1

[VV92] VILLASENOR J., VINCENT A.: An algorithm for space recognition and time tracking of vorticity tubes in turbulence. *CVGIP: Image Understanding 55*, 1 (1992), 27 – 35. 3

[WAB06] WAUGH D. W., ABRAHAM E. R., BOWEN M. M.: Spatial variations of stirring in the surface ocean: A case study of the tasman sea. *J. Phys. Oceanogr.36*, 3 (2006), 526 – 542. 3

[WC10] WOLFE C. L., CESSI P.: What Sets the Strength of the Middepth Stratification and Overturning Circulation in Eddying Ocean Models? *J. Phys. Oceanogr.40*, 7 (2010), 1520–1538. 9

[Wei91] WEISS J.: The dynamics of enstrophy transfer in two-dimensional hydrodynamics. *Physica D: Nonlinear Phenomena 48*, 2-3 (1991), 273 – 294. 3

[YNQ*10] YIM B. Y., NOH Y., QIU B., YOU S. H., YOON J. H.: The vertical structure of eddy heat transport simulated by an eddy-resolving ogcm. *Journal of Physical Oceanography 40*, 2 (2010), 340–353. 4

[ZM95] ZHU Z., MOORHEAD R. J.: Extracting and visualizing ocean eddies in time-varying flow fields, 1995. 3